doi.org/10.36721/PJPS/2026.40.16391.1

UHPLC–MS-based characterization of the pharmacokinetics and *in-vivo* metabolic profile of oleanonic acid in rats

Ruiqi Wang[1,2], Xiaoman Lou[1,2], Nigare Abuduwaili[1,2] and Yongqiang Liu[1]*

[1]State Key Laboratory Basis of Xinjiang Indigenous Medicinal Plants Resource Utilization, Key Laboratory of Chemistry of Plant Resources in Arid Regions, Xinjiang Technical Institute of Physics and Chemistry, Chinese Academy of Sciences, Urumqi 830011, PR. China

[2]University of Chinese Academy of Sciences, No. 19 (A) Yuquan Road, Shijingshan District, Beijing 100049, PR China

Abstract: **Background**: Oleanonic acid (ONA), a pentacyclic triterpenoid with significant hypoglycemic and neuroprotective activities, shows promise as a multi-target anti-diabetic candidate. However, its pharmacokinetic behavior and metabolic fate *in-vivo* remain incompletely characterized, limiting dose optimization and clinical translation. **Objective**: To investigate the pharmacokinetic profile, absolute bioavailability and metabolic pathways of ONA in rats following oral and intravenous administration. **Methods**: *In-silico* ADME predictions (SwissADME, GLORYx) were initially performed to guide the experimental design. Healthy male Sprague-Dawley (SD) rats were administered ONA either orally (36.66 mg/kg) or intravenously (3.75 mg/kg). A validated UHPLC–MS/MS method was utilized for pharmacokinetic quantification, while UHPLC–Q–Exactive Orbitrap HRMS was employed for comprehensive metabolite profiling in biological matrices. **Results**: Ten metabolites were identified, with the parent compound and metabolites predominantly detected in feces. After oral administration, ONA exhibited a C_{max} of 441.43 ± 111.09 ng/mL at t_{max} 1.3 h, $t_{1/2}$ of 1.38 ± 0.61 h, an $AUC_{0-\infty}$ of 1027.29 ± 399.45 h·ng/mL and absolute bioavailability of 12.6%. Intravenous administration showed rapid systemic clearance (CL_{obs} = 4.64 ± 0.86 L/h/kg), a large apparent volume of distribution (V_{obs} = 10.13 ± 5.16 L/kg) and an $AUC_{0-\infty}$ of 831.20 ± 154.99 h·ng/mL, consistent with extensive tissue distribution of lipophilic triterpenes. **Conclusion**: ONA exhibits low oral bioavailability, rapid clearance and extensive metabolism in rats. Fecal excretion represents a major detectable elimination route for ONA and its metabolites. These findings provide essential ADME information to support the rational development and formulation optimization of ONA-based therapeutics.

Keywords: Metabolism; Pharmacokinetics; Triterpenes; UHPLC–MS/MS

Submitted 04-03-2026 – Revised 13-04-2026 – Accepted 05-05-2026

INTRODUCTION

Diabetes is one of the most rapidly growing global health problems in the 21st century, with 589 million cases worldwide in 2024 projected to reach 853 million by 2050 (Genitsaridi *et al.*, 2026; Mossi *et al.*, 2026). Current therapeutic strategies primarily target glycemic control but often inadequately address the multifactorial nature of metabolic dysfunction and associated complications, driving the need for multi-target interventions with improved safety profiles.

Natural products represent an indispensable reservoir of innovative antidiabetic agents (Mustafa *et al.*, 2016). Oleanonic acid (ONA), widely found in medicinal plants such as *Ziziphus jujuba* and *Pistacia lentiscus* (Assimopoulou and Papageorgiou, 2005; Kawabata *et al.*, 2017; Pachi *et al.*, 2020), exhibits potent *α*-glucosidase inhibition, insulin-sensitizing activity and anti-inflammatory effects (Giner-Larza *et al.*, 2001; Harley *et al.*, 2022). These multi-target pharmacological attributes render ONA a promising candidate for comprehensive diabetic therapeutics. Additionally, its neuroprotective activity suggests potential therapeutic efficacy against diabetic cognitive impairment, as brain insulin resistance and IGF-1 resistance have been directly linked to cognitive decline in both diabetic and Alzheimer's disease patients (Talbot *et al.*, 2012).

Although accumulating evidence underscores the broad pharmacological significance of ONA, systematic investigations into its *in-vivo* pharmacokinetic characteristics remain sparse (Atanasov *et al.*, 2021). While structurally analogous triterpenes (such as oleanolic, dihydro-oleanolic and ursolic acids) are known to exhibit low oral bioavailability, rapid elimination and predominant fecal excretion, comparable pharmacokinetic and metabolic data for ONA have yet to be established (Jeong *et al.*, 2007; Chen *et al.*, 2017; Ren *et al.*, 2021; Khwaza and Aderibigbe, 2024). As a critical active site, the oxidation state of the C-3 position of pentacyclic triterpenes significantly influences pharmacological activity and metabolic stability. Specifically, the ketone group at the C-3 position of ONA differs from the hydroxyl group in oleanolic acid and ursolic acid, which confers distinct physicochemical properties, thereby impeding the direct extrapolation of pharmacokinetic and metabolic parameters (Rali *et al.*, 2016; Similie *et al.*, 2024). Clarifying these parameters is essential for dose

**Corresponding author:* e-mail: liuyq@ms.xjb.ac.cn

Article in Press

optimization, formulation design and clinical translation. Modern UHPLC–MS/MS and UHPLC–HRMS techniques enable reliable quantification and metabolite identification for lipophilic compounds. Sprague-Dawley (SD) rats are a widely recognized standardized rodent model in preclinical pharmacokinetic and drug metabolism studies. This model has been well established for evaluating drug absorption, distribution and biotransformation and is suitable for characterizing the pharmacokinetic profile and metabolic spectrum of ONA.

Against this background, this study aims to systematically explain the pharmacokinetic behavior and metabolites of oleanonic acid (ONA) in rats by integrating *in-silico*-aided prediction, metabolite analysis based on UHPLC–HRMS and quantitative analysis methods based on UHPLC–MS/MS.

MATERIALS AND METHODS

Materials

Acetonitrile, formic acid and methanol were all LC−MS grade. Oleanonic acid and ursolic acid standards (purity ≥ 98%) were supplied by Wuhan Zhongbiao Technology Co., Ltd. (Wuhan, China). Ethanol and distilled water used in the experiment were analytically pure. Kolliphor® EL was supplied by Sigma-Aldrich (St. Louis, MO, USA).

Instruments

For metabolite identification, chromatographic separation was performed on a Dionex UltiMate 3000 RSLC system (Thermo Fisher Scientific, Waltham, MA, USA) and mass spectrometric detection was carried out on a Q Exactive Plus Orbitrap mass spectrometer (Thermo Fisher Scientific, Waltham, MA, USA).

For quantitative analysis, chromatographic separation was conducted on an ExionLC UHPLC system (SCIEX, Framingham, MA, USA) and mass spectrometric detection was performed on a QTRAP 6500^{+} mass spectrometer (SCIEX, Framingham, MA, USA).

In-silico ADME and metabolic predictions

To preliminarily evaluate the pharmacokinetic and metabolic properties of ONA, *in-silico* predictions experiments were carried out before conducting *in-vivo* research (Lipinski *et al.*, 2001). The GLORYx platform can simulate potential biotransformation sites. The SwissADME platform can predict the key physicochemical properties of compounds and the key pharmacokinetic parameters (Daina, Michielin and Zoete, 2017; de BruynKops *et al.*, 2021). The computer simulation process aimed to provide a theoretical framework for the metabolic spectrum of ONA and to guide the rapid identification of ONA metabolites in complex biological matrices. These results collectively laid the theoretical foundation for the design of subsequent experiments.

Animals, preparation and pharmacokinetic study

Ethical declaration and animal handling: All animal experiments were permitted by the Ethics Committee of Xinjiang Medical University (approval No. IACUC-JT-20250626-01). Ten healthy male Sprague–Dawley (SD) rats (7–8 weeks old, 200 ± 20 g) were used for the pharmacokinetic study. The rats were housed on the same rack in a temperature-controlled room (25 ± 2 °C) under a 12 h light/12 h dark cycle, with free access to food and water, to minimise environmental variability. The rats were assigned to two groups (n = 5 per group) by simple manual allocation. Each individual rat served as an experimental unit. As the primary objective of this study was to evaluate the absolute oral bioavailability of ONA by comparing oral and intravenous administration, blank plasma collected before ONA administration was used as the control sample. The sample size (n = 5 per group) was determined based on common experimental practices for exploratory rodent pharmacokinetic studies. All 10 animals (n = 5 per group) completed the study and no animals, experimental units, or data points were excluded from the pharmacokinetic analysis. Five male Sprague–Dawley (SD) rats (7–8 weeks old, 200 ± 20 g) were used for metabolite profiling. The housing conditions and ethical procedures were consistent with those described above to minimise environmental variability. Healthy male SD rats were included in the study and no explicit exclusion criteria were established a priori. Animals were monitored daily for health status and behavioral changes. No unexpected adverse events, severe distress, or signs of toxicity were observed during the study period. During the procedures of intragastric administration, intravenous injection and blood collection, gentle handling was carried out on the experimental animals to minimize their pain, suffering and stress responses.

Formulation Preparation: In animal experiments, ONA was prepared in the form of oil-in-water (O/W) emulsion to optimize solubility. ONA powder was ground with a small amount of anhydrous ethanol and Kolliphor® EL was added dropwise. The mixture was ground continuously until uniform and distilled water was added with continuous grinding. Oral (36.66 mg/kg) and intravenous (3.75 mg/kg) preparations were freshly prepared and visual inspection was carried out before administration to ensure uniformity. According to the pharmacokinetic profiles of structurally related oleanane-type triterpenes, a dose ratio of approximately 10:1 (oral versus intravenous) was adopted. OA differed from ONA solely at the C-3 position (The ketone group replaces the hydroxyl group), yet its oral bioavailability was exceedingly low (0.7% in rats) (Jeong *et al.*, 2007). A comparable pharmacokinetic pattern was also reported for dihydro-oleanolic acid (Chen *et al.*, 2017). Given their comparable lipophilicity, ONA was expected to show similarly poor oral absorption. The selected oral dose (36.66 mg/kg) fell within the pharmacologically

Article in Press

effective range (15–60 mg/kg) in diabetic rats (Harley *et al.*, 2022). The intravenous dose (3.75 mg/kg) ensured quantifiable plasma concentrations over 24 h. This experimental design facilitated the accurate determination of absolute bioavailability and the detection of metabolites via UHPLC–HRMS.

Pharmacokinetic study design: The oral group received ONA (36.66 mg/kg) via gavage, with blood samples collected at 0, 0.25, 0.5, 1, 1.5, 3, 6, 9, 12 and 24 h post-dose. The intravenous injection group was given ONA (3.75 mg/kg) via tail vein injection and orbital blood samples were collected at 0.08, 0.25, 0.5, 1, 1.5, 3, 6, 9, 12 and 24 h. Blood was collected in EP tubes containing anticoagulant and centrifuged for 15 min at a speed of 3,000 rpm to separate plasma. Plasma samples were stored at −80ºC for analysis. No formal blinding was performed during group allocation, drug administration, or sample collection, as pharmacokinetic evaluation relies on objective quantitative analysis via UHPLC–HRMS.

Metabolic product research: SD rats were orally administered a single dose of ONA at 36.66 mg/kg. Urine and fecal samples were collected separately from the animals using individual metabolic cages during 0–24 h after administration and stored at −80 °C until metabolite analysis. Before administration, 24h blank urine and fecal samples were collected from the rats and processed as described above.

Preparation of samples and standards

Preparation of reserve and working solutions: ONA (5 mg) was precisely weighed and dissolved in 1 mL DMSO to make a 5 mg/mL ONA stock solution. The solution was diluted stepwise with methanol to obtain the standard curve and the working solution for QC samples. The preparation method of the internal standard (IS) stock solution (ursolic acid) was the same and the concentration was prepared at 5 μg/mL. To 100 μL of blank rat plasma, 10 μL of ONA working solution at different concentrations and 10 μL of IS solution were added. After vortex mixing, 300 μL of acetonitrile was added for protein precipitation. The samples were centrifuged and the supernatants were filtered through a 0.22 μm membrane filter to obtain the calibration standard samples.

Preparation of QC samples: 10 μL working solution was added to 100 μL blank rat plasma and then mixed by vortex for 30 s, followed by the same protein precipitation and filtration procedures. The QC samples were constituted at low (50 ng/mL), medium (500 ng/mL) and high (2500 ng/mL) concentrations.

Preparation of plasma samples: Plasma (100 μL) was mixed with 10 μL of methanol and 10 μL of IS (5000 ng/mL) and vortexed for 3 s after each addition. Acetonitrile (300 μL) was added for protein precipitation, followed by vortexing for 60 s. After 7 minutes of centrifugation at 14,000 rpm, the supernatant was used for chromatographic experiments.

Excreta Sample Preparation: Pooled feces (10 g) or urine (15 mL) from five rats were extracted with acetonitrile (30 mL for feces; 45 mL for urine) via 30 min ultrasonication and centrifuged (5,000 rpm, 10 min). The supernatants were rotary-evaporated to dryness and reconstituted in methanol (4 mL for feces; 2 mL for urine). After 1 min vortexing and centrifugation (14,000 rpm, 7 min; 4ºC), the supernatants were filtered (0.22 μm), N_2-dried at 25ºC and finally reconstituted in 100 μL methanol for analysis.

UHPLC–HRMS for metabolite identification

The chromatography column was CORTECS® C18+ (2.7 μm, 2.1 × 75 mm). The gradient mobile phase consisted of 0.1% formic acid in water (A) and acetonitrile (B), with the column temperature set at 40ºC and the injection volume set at 2 μL. The elution gradient program was as follows: 0–3 min, 40.0% B at 150 μL/min; 3–13 min, 40.0% B with linear flow increase to 300 μL/min; 13–53 min, 40.0–60.0% B; 53–113 min, 60.0–80.0% B; 113–114 min, 80.0–100.0% B; 114–115 min, 100.0% B. From 13 min onward, flow velocity was maintained at 300 μL/min. The probe temperature was 350ºC and the capillary temperature 320 ºC. The S-Lens RF level was adjusted to 55 and the sheath pressure was maintained at 40 arb. Ionization conditions were optimized as follows: spray voltage +3.2 kV/−2.8 kV, collision energy 20/40/60 (+) and 40/55/70 (−). Auxiliary gas flow was adjusted according to the ionization mode, which was 10 arb under positive ionization and 15 arb under negative ionization. Within the *m/z* range of 100–1500, full-scan MS/dd-MS^2 analysis was performed at a resolution of 70,000 FWHM and MS^2 analysis was performed at a resolution width of 17,500 FWHM (4 Da isolation). Data were processed using Xcalibur 4.7.

UHPLC–MS/MS conditions for quantitative analysis

The chromatography column was CORTECS® C18+ (2.7 μm, 2.1 × 75 mm) and the column temperature was the same as described above. The isocratic mobile phase consisted of 17% 0.1% formic acid in water (A) and 83% acetonitrile (B), at a flow rate of 250 μL/min and an injection volume of 5 μL. MRM was conducted in negative ESI mode using the mass spectrometer. The operating conditions were: spray voltage, −4.5 kV; ion source temperature, 450ºC. The MRM pairs monitored were *m/z* 453.3/407.5 for ONA (declustering potential −122 V, collision energy −52 V) and *m/z* 455.3/407.3 for the internal standard (declustering potential −147 V, collision energy −56 V). Ursolic acid (UA) and oleanonic acid (ONA) are both pentacyclic triterpenoids with comparable molecular weights (ONA: 454.68 Da; UA: 456.70 Da) and similar high lipophilicity. Their chromatographic retention behaviors are comparable without mutual interference in mass spectrometric detection, thus UA was selected as the internal standard. Data acquisition was performed using Analyst 1.7 and the data were subsequently processed

Article in Press

using SCIEX OS-MQ 3.16.44. The pharmacokinetic parameters were calculated using MaS Studio 1.6.2.1.

Method validation

Method validation was conducted following FDA guidance (U.S. Food and Drug Administration, 2018), covering selectivity, linearity, accuracy, precision, recovery, matrix effect and stability.

Selectivity

Chromatographic analysis of blank plasma from six sources, plasma spiked with ONA and IS and post-dose samples with IS was performed to assess specificity.

Linearity

To evaluate linearity, calibration standards covering the ONA concentration range were prepared. Peak area ratios (ONA/IS) were quantified using $1/x^2$ weighted least squares regression. Linearity was assessed by r^2. LLOQ was defined as the lowest calibration concentration with $S/N \geq 10$.

Matrix effect and recovery

Extraction recovery and matrix effect were assessed using QC samples at three concentrations. For ONA, both parameters were calculated via the internal standard (IS) normalization method to reduce variations in extraction efficiency and instrument response. Extraction recovery was determined as the ratio of ONA/IS peak areas in pre-extraction spiked samples to those in post-extraction spiked samples. Matrix effect was expressed as the ratio of ONA/IS peak areas in post-extraction spiked samples to those in pure standard solutions, representing the IS-normalized matrix factor. The extraction recovery and matrix effect of IS itself were calculated based on its absolute peak area.

Precision and accuracy

The accuracy and precision of the method were verified by three levels of QC samples. Six replicate samples at each level were analyzed on a single day to determine intra-day precision and over three separate days to assess inter-day precision. Accuracy and precision were expressed as RE and RSD, respectively. According to FDA guidelines, the RE and RSD values for all batches should be within ±15%.

Stability

Stability was systematically studied using QC samples at three levels under four conditions. Short-term stability was assessed by storing samples at room temperature for 12 h, long-term stability at −80 ºC for 7 days and freeze-thaw stability through three cycles between −80 ºC and room temperature. Processed sample stability was also evaluated for 12 h in the autosampler (15 ºC). Acceptance criteria required RE and RSD within ±15%, per FDA bioanalytical guidance.

RESULTS

In-silico metabolism and pharmacokinetic prediction

Systematic *in-silico* prediction of potential metabolic sites and biotransformation pathways for ONA was performed using the GLORYx platform (Fig. 1) (de BruynKops *et al.*, 2021; Pelletier *et al.*, 2025). The prediction results demonstrated that ONA was prone to Phase Ⅰ and Phase Ⅱ metabolic reactions and the high probability metabolic sites were distributed in multiple positions of the pentacyclic triterpene skeleton. The prediction results demonstrated that the carbonyl group at C-3 in Phase I metabolism was very likely to have a reduction reaction. In addition, several carbon atoms in the triterpene skeleton would undergo hydroxylation. In Phase II metabolism, the computer predicted that *O*-glucuronidation was likely to occur on the carboxylic acid functional group of ONA.

Swiss ADME was used to predict the physicochemical properties and ADME parameters of ONA (Table 1). ONA showed a relatively high molecular weight (454.68 Da) and pronounced lipophilicity, with a Log *P* value of 6.11, exceeding the typical threshold defined by Lipinski's five rules. ONA was hydrophobic and multiple solubility prediction models classified ONA as an insoluble substance. Swiss ADME predicted that the gastrointestinal absorption rate of ONA was low and lacked blood-brain barrier (BBB) permeability. In addition, it was predicted that ONA was not a P-glycoprotein (P-gp) substrate, but showed the potential inhibitory activity against CYP2C9.

In-vivo metabolic profiling and metabolite identification of ONA

After oral administration of ONA to rats, biological samples including urine, feces and plasma were collected and the metabolic spectrum of ONA in the body was comprehensively evaluated by high-resolution mass spectrometry combined with chromatography (Takahashi *et al.*, 2018). In the process of metabolite identification, data were collected in both ionization modes. The negative ion mode provided high-intensity precursor ions and the positive ion mode produced rich characteristic ion fragments through extensive dissociation. Therefore, this complementary double ionization strategy was used: the positive ion mode was used for structural analysis and the negative ion mode was used for quantitative detection. This method enabled comprehensive analysis of ONA-derived metabolites in complex biological matrices.

In order to identify metabolites, the fragmentation pattern of ONA was first characterized by using the positive ion mode of HRMS (Uddin *et al.*, 2022). The *m/z* of the protonated molecular ion $[M+H]^+$ was 455.3523 (calculated for $C_{30}H_{47}O_3$). Its characteristic fragmentation pathway was dehydration to produce a fragment ion with *m/z* of 437.3413.

Article in Press

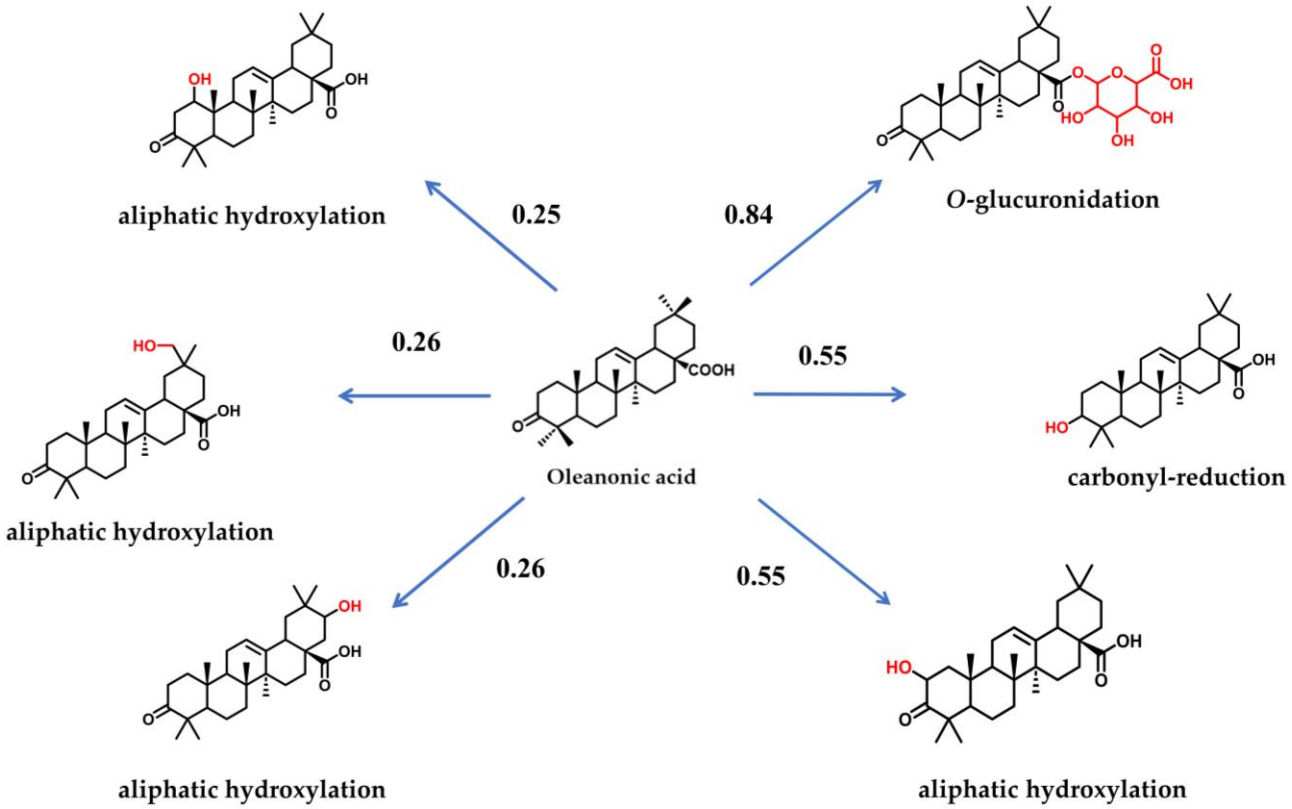

Fig. 1: *In-silico* metabolic site prediction and probability scoring of ONA using GLORYx.

Table 1: Physicochemical, pharmacokinetic, and ADME properties of ONA predicted by SwissADME

Parameter	Predicted value
Molecular weight (Da)	454.68
Consensus Log *P*	6.11
ESOL solubility class	Poorly soluble
Ali solubility class	Poorly soluble
GI absorption	Low
BBB permeant	No
P-gp substrate	No
CYP2C9 inhibitor	Yes
Bioavailability score	0.85

Note: Log *P*, octanol–water partition coefficient; ESOL, estimated solubility; Ali, Ali's solubility model; GI, gastrointestinal; BBB, blood–brain barrier; P-gp, P-glycoprotein; CYP, cytochrome P450; Bioavailability score, probability of achieving >10% oral bioavailability in rats.

In addition, obvious fragment ions were observed at *m/z* 409.3465, corresponding to the loss of 46 Da from the precursor ion. This loss of neutrality may be attributed to the decarboxylation reaction accompanied by skeletal rearrangement. This is a common phenomenon of triterpenic acid cleavage. In addition, diagnostic retro-Diels-Alder (RDA) fragment ions at *m/z* 203.1796 were also detected, which are widely regarded as characteristic fragment ions of pentacyclic triterpene compounds (Fig. 2).

UHPLC–Q-Exactive Orbitrap HRMS analysis revealed the unique distribution patterns of ONA and its metabolites in biological matrices (Table 2). Except for M6a, all preliminarily identified metabolites were characterized in positive ion mode. M6a (*O*-glucuronide) was preliminarily identified under the condition of negative ion mode (Kostiainen *et al.*, 2003). ONA (M0) in plasma was mainly detected in the form of parent compound and no Phase I or Phase II metabolites higher than the analysis threshold were observed. No ONA-related substances were detected in urine. Feces were the main route of elimination for parent compound and their metabolites.

From the detected metabolites, the ONA metabolic pathway was established (Table 2).

Article in Press

Table 2: Identification of ONA metabolites in rat biological samples by high-resolution UPLC–Orbitrap mass spectrometry

Metabolite	Matrix	t_R (min)	Ion mode	Observed *m/z*	Calculated *m/z*	Mass error (ppm)	Molecular formula	Biotransformation	MS/MS fragments (*m/z*)
M0	Plasma feces	56.61	$[M+H]^+$	455.3516	455.3519	−1.63	$C_{30}H_{46}O_3$	——	437.3408,409.3467,203.1799
M1a	Feces	4.57	$[M+H]^+$	453.3364	453.3363	0.24	$C_{30}H_{44}O_3$	Dehydrogenation	435.3250,407.3313,201.1638,189.1642
M1b	Feces	37.82	$[M+H]^+$	453.3362	453.3363	−0.31	$C_{30}H_{44}O_3$	Dehydrogenation	435.3260,407.3317,201.1640,189.1640
M2a	Feces	47.38	$[M+H]^+$	457.3671	457.3676	−1.08	$C_{30}H_{48}O_3$	Reduction	439.3583,411.3633,189.1645
M2b	Feces	49.57	$[M+H]^+$	457.3673	457.3676	−0.75	$C_{30}H_{48}O_3$	Reduction	439.3588,411.3621,203.1804
M3a	Feces	16.10	$[M+H]^+$	471.3468	471.3469	−1.28	$C_{30}H_{46}O_4$	Oxidation	425.3416,407.3321,201.1639
M3b	Feces	31.41	$[M+H]^+$	471.3468	471.3469	−0.18	$C_{30}H_{46}O_4$	Oxidation	453.3365,435.3257,407.3307,201.1639
M4a	Feces	10.90	$[M+H]^+$	473.3625	473.3625	−0.04	$C_{30}H_{48}O_4$	Hydration	455.3531,409.3470,203.1796
M5a	Feces	16.25	$[M+H]^+$	437.3416	437.3414	0.33	$C_{30}H_{44}O_2$	Dehydration	391.3343,201.1639
M5b	Feces	33.37	$[M+H]^+$	437.3409	437.3414	−1.14	$C_{30}H_{44}O_2$	Dehydration	391.3359,201.1639,189.1639
M6a	Feces	27.31	$[M-H]^-$	629.3696	629.3684	1.94	$C_{36}H_{54}O_9$	*O*-glucuronidation	453.3376,407.3309

Note: Parent drug(M0), Dehydrogenation (M1), Reduction (M2), Oxidation (M3), Hydration (M4), Dehydration (M5), *O*-glucuronidation (M6)

ONA underwent a variety of Phase I biotransformations in rats, including dehydrogenation (M1), reduction (M2), oxidation (M3), hydration (M4) and dehydration (M5) and then underwent Phase II conversion via *O*-glucuronidation (M6). The reduction reaction (M2) produced two isomeric metabolites (M2a and M2b) and the mass increased by 2 Da. The mass of metabolites produced by oxidation reaction (M3) and hydration reaction (M4) increased by 16 Da and 18 Da, respectively. The mass of dehydrated product (M5) decreased by 18 Da and the mass of *O*-glucuronidated metabolite (M6a) increased by 176 Da.

Methodological validation

Selectivity

The selectivity of the method was evaluated by the following four sample sets: (A) Blank rat plasma; (B) spiked calibration sample (ONA and IS); (C) 3 h post-oral ONA samples with IS; (D) 3 h post-injection ONA samples with IS. As shown in Fig. 3, analyte and IS retention windows were free from endogenous matrix interference in all blank runs.

Linearity

This method showed a good linear relationship in the range of 5–5000 ng/mL. The obtained correlation coefficient (r^2) was greater than 0.997. The concentration of 5 ng/mL was defined as LLOQ. At this concentration, the *S/N* of ONA exceeded 10.

Precision and accuracy

For intra-day evaluation, the RSD value of this method was 3.78–5.62% and the RE value ranged from -4.97% to 6.98% (Table 3). For the inter-day assessment, the RSD value of all three concentration levels was less than 5.64% and the RE value ranged from -4.35% to 8.93%. All the results met the acceptance criteria of ±15% per FDA guidance, indicating that the established negative ion mode had excellent precision and accuracy and fully met the requirements of research.

Recovery and matrix effect

Regarding the extraction recovery, the average recovery of ONA ranged from 89.50% to 106.00% and the RSD at each level was less than 15%. The average extraction recovery of the IS was 101.93% (RSD 7.03%). The IS-normalized matrix factors of ONA at three QC levels were 98.00%, 103.94% and 92.50%, respectively and the RSD values were $\leq$ 8%, indicating that the internal standard compensated for the matrix effect to a certain extent.

The absolute matrix effect was 110.87% (RSD 1.88%), indicating the existence of ion enhancement (Table 4). These results met the acceptance standards of biological analysis method verification, indicating that the protein precipitation method enabled efficient and reproducible extraction of the target compound from plasma.

e in Press

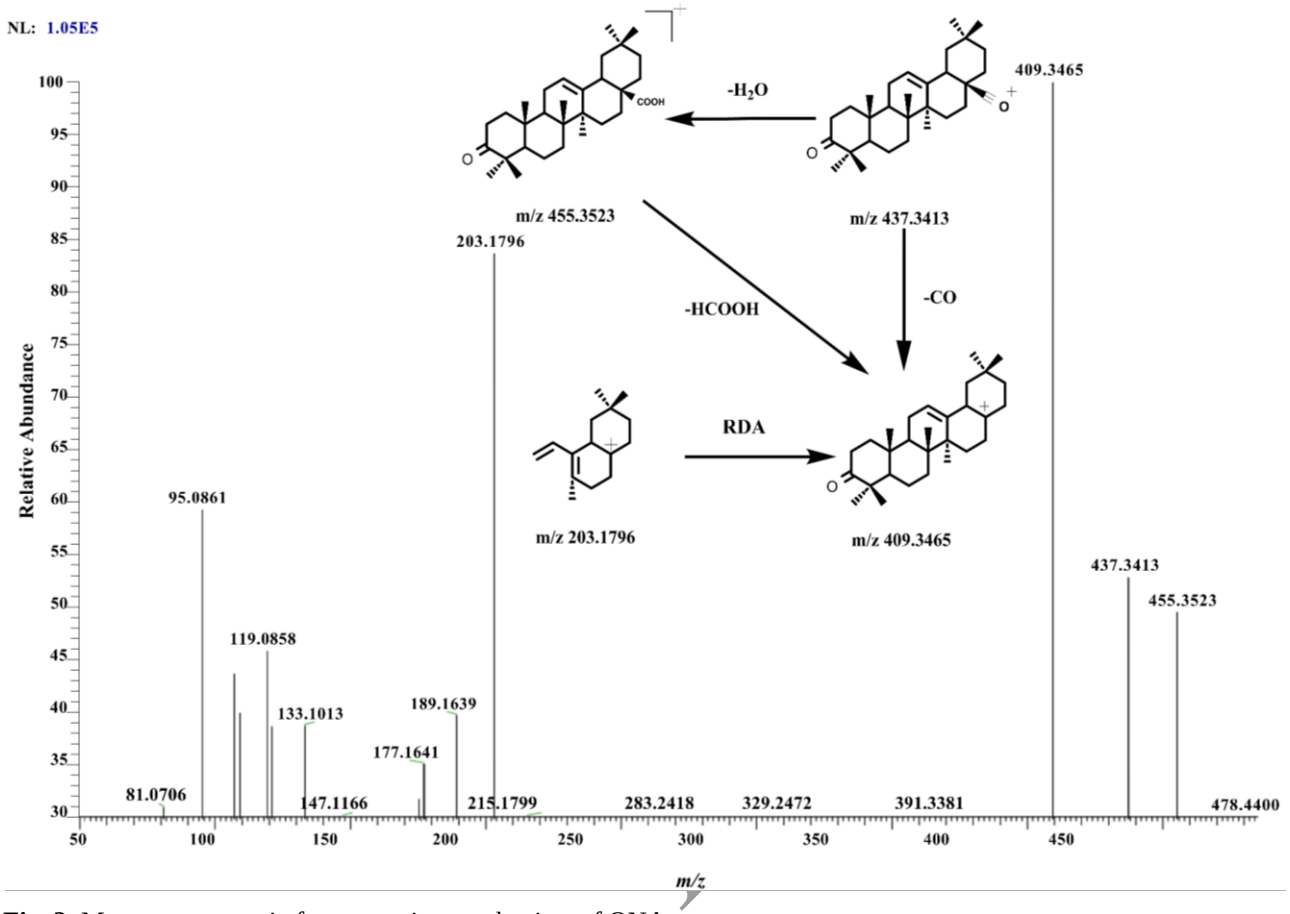

Fig. 2: Mass spectrometric fragmentation mechanism of ONA.

Stability

Table 5 summarized the results of samples under various conditions. The results showed that under four key storage and processing conditions, the relative error (RE) of ONA concentration ranged from -13.35% to 11.69% and all RSD values were ≤ 15%. Specifically, ONA in the plasma samples remained stable after 12 hours of storage at room temperature and after three freeze-thaw cycles. For processed samples, after 12 hours of storage in an autosampler (15℃), the change in ONA concentration remained within an acceptable range. In addition, there was no obvious change in the concentration after a week of long-term storage at -80℃. Collectively, these results showed that ONA had acceptable chemical stability during the experiment.

Pharmacokinetic characteristics and bioavailability of ONA in rats

Pharmacokinetic parameters of oleanonic acid (ONA) were calculated using non-compartmental analysis with the linear up/log down trapezoidal method and extrapolation to infinity. After oral and intravenous injection, ONA exhibited rapid systemic clearance (Fig.4). The half-life after oral administration was 1.38 hours and the half-life after intravenous injection was 1.47 hours. The corresponding $AUC_{0-\infty}$ values were 1027.29 ± 399.45 h·ng/mL (oral) and 831.20 ± 154.99 h·ng/mL (intravenous), respectively. The absolute oral bioavailability was 12.6% (Table 6). After intravenous administration, the volume of distribution (V_{obs} = 10.13 L/kg) and systemic clearance (CL_{obs} = 4.64 L/h/kg) indicated extensive tissue distribution and efficient hepatic extraction.

DISCUSSION

This study established an *in-silico*-aided experimental workflow integrating computational ADME prediction, UHPLC–MS/MS-based pharmacokinetic quantification, UHPLC–HRMS metabolite profiling and excretion analysis to systematically characterize the *in-vivo* disposition characteristics of oleanonic acid (ONA) in rats. Predictions from GLORYx and SwissADME indicated that ONA exhibited high lipophilicity and poor aqueous solubility and primarily underwent Phase I reduction/oxidation reactions followed by Phase II glucuronidation. These predictions were generally consistent with the experimental results, supporting the predictive value of computational tools in natural product metabolism research and demonstrating their utility as effective means for preliminary screening and experimental design optimization in metabolism studies (Daoud *et al.*, 2021).

Article

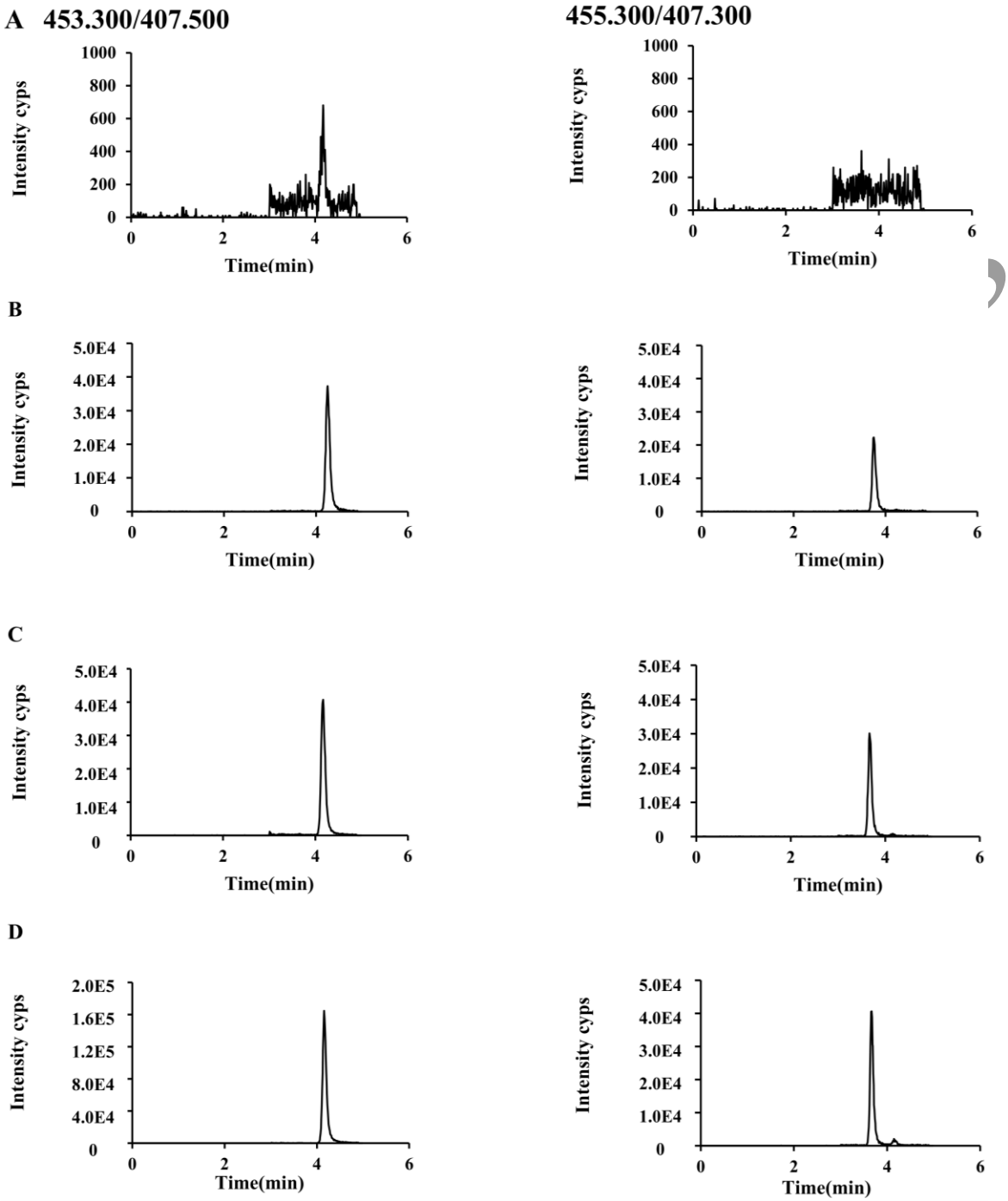

Fig. 3: Representative MRM chromatograms of ONA and the internal standard (IS) in rat plasma. (A) Blank rat plasma; (B) spiked calibration sample (ONA and IS); (C) actual plasma sample collected at 3 h after oral administration of ONA (36.66 mg/kg); and (D) actual plasma sample collected at 3 h after intravenous injection of ONA (3.75 mg/kg).

Table 3: Precision and accuracy of ONA in rat plasma under intra-day and inter-day conditions

Analytes	Nominal conc. ng/mL	Intra-day mean	RSD (%)	RE (%)	Inter-day mean	RSD (%)	RE (%)
ONA	50	53.49	5.62	6.98	54.47	5.64	8.93
	500	514.91	3.78	2.98	511.34	3.79	2.26
	2500	2375.82	4.82	−4.97	2391.25	5.60	−4.35

Table 4: Extraction recovery and matrix effect of ONA in rat plasma

Analytes	Nominal conc. ng/mL	Recovery (%)		Matrix effect (%)	
		Mean± SD	RSD	Mean± SD	RSD
ONA	50	102.68 ± 2.93	2.86	98.00 ± 1.11	1.13
	500	89.50 ± 5.67	6.32	103.94 ± 8.29	7.98
	2500	106.00 ± 12.45	11.74	92.50 ± 3.86	4.18
IS	500	101.93 ± 7.17	7.03	110.87 ± 2.08	1.88

Table 5: Evaluation of ONA stability in rat plasma under different storage conditions

Storage condition	Nominal conc. ng/mL	Mean (ng/mL)	RE (%)	RSD (%)
Short-term (Room temperature for 12 h)	50	53.51	7.01	5.64
	500	497.67	− 0.47	2.73
	2500	2469.84	− 1.21	8.75
Autosampler (15°C for 12h)	50	55.85	11.69	1.50
	500	491.77	− 1.65	3.39
	2500	2391.24	− 4.35	10.24
Freeze-thaw (3cycles −80°C to room temperature)	50	47.97	− 4.06	14.99
	500	470.33	− 5.93	9.95
	2500	2219.43	− 11.22	2.13
Long-term stability (−80°C, 7days)	50	45.17	− 9.65	5.22
	500	433.24	− 13.35	1.56
	2500	2203.61	− 11.86	3.35

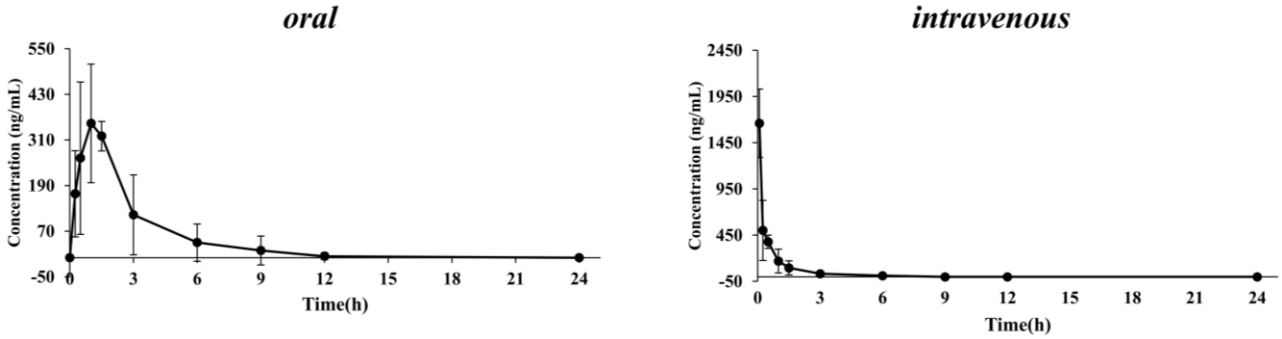

Fig. 4: Mean plasma concentration-time profiles of ONA in rats following a single oral (36.66 mg/kg) and intravenous (3.75 mg/kg) administration

Table 6: Pharmacokinetic evaluation of ONA in rats under oral and intravenous administration conditions

Parameter	Units	Oral (36.66 mg/kg)	Intravenous (3.75 mg/kg)
$t_{1/2}$	h	1.38 ± 0.61	1.47 ± 0.63
T_{max}	h	1.3	——
C_{max}	ng/mL	441.43 ±111.09	1660.28 ± 371.03
AUC_{0-t}	h·ng/mL	1014.73± 405.49	798.72 ± 155.73
$AUC_{0-\infty}$	h·ng/mL	1027.29± 399.45	831.20 ± 154.99
CL_{obs}	L/h/kg	39.15 ±11.48	4.64 ± 0.86
V_{obs}	L/kg	70.90 ± 7.97	10.13 ± 5.16
F	%	12.6%	——

Note: $t_{1/2}$: half-life; Tmax: time to maximum concentration; C_{max}: maximum concentration; AUC_{0-t}: area under the curve from 0 to last sampling; $AUC_{0-\infty}$: area under the curve extrapolated to infinity; CL_{obs}: observed clearance; V_{obs}: observed volume of distribution; F: absolute bioavailability.

Given the complex and diverse structures of pentacyclic triterpenoids, this workflow provided a valuable reference framework for metabolite screening and mass spectrometry analytical strategy optimization.

A dual-polarity UHPLC–HRMS strategy was applied for the analysis of triterpenoid metabolites. The positive ion mode provided abundant fragment ions that facilitated structural elucidation, whereas the negative ion mode

Article Press

offered higher sensitivity for conjugated metabolites such as glucuronides. The complementary use of both ionization modes improved metabolite coverage and identification confidence. This approach has been applied in the metabolic profiling of triterpenoid compounds. Ten metabolites were tentatively identified, which were consistent with multiple metabolites predicted by *in-silico* tools, indicating that ONA underwent Phase I biotransformation reactions (reduction, hydroxylation, dehydrogenation), followed by Phase II *O*-glucuronidation reactions. Phase I modifications mainly occurred at the A-ring and the C-3 ketone group, suggesting that this structural feature may be associated with the susceptibility of ONA to reductive biotransformation. Compared with oleanolic acid (OA), both ONA and OA contain a C-28 carboxyl group that may undergo glucuronidation at this site (e.g., M6a detected in this study, +176 Da, which is likely a conjugate of this type). The main structural difference between them lies at the C-3 position (ONA has a ketone group while OA has a hydroxyl group) and this difference may affect Phase I metabolic pathways to some extent, contributing to the increased reductive reactions observed in ONA. These results suggested that molecular structural differences may influence metabolic behavior. The C-3 ketone moiety in ONA may contribute to distinct Phase I metabolic profiles compared to the C-3 hydroxyl in oleanolic acid; however, the specific effect on individual pathways remains to be further elucidated. In addition, ONA and its metabolites were mainly detected in fecal samples and no parent drug or metabolites were detected in urine. This distribution pattern may be related to its limited absorption and potential hepatobiliary excretion and/or intestinal metabolism, but the specific elimination mechanism needs to be verified by further quantitative excretion studies. This phenomenon is generally consistent with reports on other highly lipophilic triterpenoids such as glycyrrhizin and suggests that enterohepatic circulation may be involved in its *in-vivo* process, which requires further investigation for confirmation (Ichikawa *et al.*, 1986; Yang *et al.*, 2009). Pharmacokinetic analysis revealed that ONA exhibited rapid clearance, extensive tissue distribution and low absolute oral bioavailability (12.6%) in rats. Following intravenous administration, the apparent volume of distribution (V_{obs} = 10.13 L/kg) was significantly higher than the total body fluid volume (approximately 0.7 L/kg in rats), reflecting extensive distribution in peripheral tissues, which was consistent with its high lipophilicity (Davies and Morris, 1993). The systemic clearance (CL_{obs} = 4.64 L/h/kg) was close to the hepatic blood flow rate in rats, suggesting that it may have a high hepatic extraction ratio. The apparent oral clearance was approximately 8-fold higher than the intravenous clearance, consistent with its low bioavailability, indicating that absorption limitation is an important factor affecting systemic exposure.

According to the Biopharmaceutics Classification System (BCS), the low aqueous solubility of ONA and its predicted low gastrointestinal absorption (SwissADME) suggested that it might exhibit characteristics similar to BCS Class IV compounds, where both solubility and permeability may limit its oral absorption (Amidon *et al.*, 1995). However, the observation that the apparent oral clearance was significantly higher than the intravenous clearance suggested that gastrointestinal dissolution may be one of the key steps limiting systemic exposure. This result indicated that formulation strategies aimed at improving solubility, such as amorphous solid dispersions or lipid nanocarriers, may help improve its oral bioavailability (Vasconcelos, Sarmento and Costa, 2007; Xi *et al.*, 2009). Certain inherent constraints of this exploratory study should be noted. To minimize hormonal fluctuations, only male rats were evaluated, leaving potential sex-specific pharmacokinetic variations to be addressed in future work. Additionally, given interspecies differences in metabolic enzymes and transporters, caution is warranted when translating these preliminary rodent findings directly to human physiology.

In summary, the low oral bioavailability of ONA may be attributed to both dissolution limitation and hepatic first-pass metabolism, consistent with the characteristics reported for structurally related pentacyclic triterpenoids such as oleanolic acid, which exhibits extremely low oral bioavailability due to poor gastrointestinal absorption and extensive hepatic metabolism in rats (Jeong *et al.*, 2007) and whose bioavailability can be markedly enhanced by lipid-based formulation strategies (Garcia-Gonzalez A *et al.*, 2023). The C-3 ketone group may enhance its propensity for biotransformation, but this hypothesis requires further experimental verification. In addition, the roles of efflux transporters (e.g., P-gp) and metabolic enzymes (e.g., CYP and UGT isoforms) in its *in-vivo* process remain to be further investigated. From an application perspective, the pharmacokinetic and metabolite data obtained in this study provided a basis for formulation optimization and suggested that improving solubility and regulating *in-vivo* exposure may be effective strategies to enhance its oral absorption.

CONCLUSION

Oleanonic acid (ONA) is a bioactive natural triterpenoid whose *in-vivo* disposition remains poorly characterized. This study established an integrated "*in-silico* prediction–high-resolution metabolite identification–*in-vivo* pharmacokinetic evaluation" strategy and a validated UHPLC–MS/MS method to systematically characterize ONA disposition in rats. SwissADME and GLORYx predicted high lipophilicity and major metabolic pathways involving reduction, oxidation and glucuronidation. UHPLC–HRMS tentatively identified 10 metabolites,

Article in Press

indicating that ONA primarily underwent Phase I biotransformations (reduction, oxidation, hydration, dehydration and dehydrogenation) and Phase II *O*-glucuronidation. Pharmacokinetic results demonstrated rapid absorption and elimination, along with low absolute oral bioavailability in rats. However, the roles of enzymes and transporters involved in ONA metabolism remain unclear and interspecies differences have not been evaluated. Future studies should further elucidate these mechanisms and explore formulation strategies to improve oral bioavailability.

Acknowledgment (AI Disclosure Statement)
During the preparation of this manuscript, Kimi and Gemini were used solely for the refinement of grammar and academic expression. The authors rigorously reviewed and revised all outputs and bear full responsibility for the accuracy, completeness and originality of the content. No artificial intelligence tools were employed for data analysis, figure generation, or scientific result production.

Authors' contributions
Ruiqi Wang: Writing-original draft, Investigation, Formal analysis, Data curation, Methodology, Validation, Visualization; Xiaoman Lou: Investigation, Software; Nigare Abuduwaili: Investigation, Methodology; Yongqiang Liu: Supervision, Resources, Writing-review and editing.

Funding
This study was financially supported by the Key Research and Development Program of Xinjiang (No. 2025B03013-1).

Data availability statement
All data generated or analysed during this study are included in this published article.

Ethical approval
All animal experiments were permitted by the Ethics Committee of Xinjiang Medical University (approval No. IACUC-JT-20250626-01). This study was performed in adherence with the ARRIVE guidelines. See supplementary file for the ARRIVE checklist.

Conflicts of interest
The authors declare no conflict of interest.

REFERENCES

Amidon GL, Lennernas H, Shah VP and Crison JR (1995). A theoretical basis for a biopharmaceutic drug classification: The correlation of *in-vitro* drug product dissolution and *in-vivo* bioavailability. *Pharm. Res.*, **12**(3): 413–420.

Assimopoulou AN and Papageorgiou VP (2005). GC-MS analysis of penta- and tetra-cyclic triterpenes from resins ofPistacia species. Part I.Pistacia lentiscus var. Chia. *Biomed. Chromatogr.*, **19**(4): 285–311.

Atanasov AG, Zotchev SB, Dirsch VM, the International Natural Product Sciences Taskforce and Supuran, C.T. (2021). Natural products in drug discovery: Advances and opportunities. *Nat. Rev. Drug Discov.*, **20**(3): 200–216.

Chen R, Li W, Li Y, Liu Y, Huang J and Tang L (2017). Study on the pharmacokinetics of oleanolic acid and dihydrooleanolic acid by intragastric administra-tion and intravenous injection in rats *in-vivo*. *China Pharm.*, **28**(13): 1777.

Daina A, Michielin O and Zoete V (2017). SwissADME: A free web tool to evaluate pharmacokinetics, drug-likeness and medicinal chemistry friendliness of small molecules. *Sci. Rep.*, **7**(1): 42717.

Daoud NEH, Borah P, Deb PK, Venugopala KN, Hourani W, Alzweiri M, Bardaweel SK and Tiwari V (2021). ADMET profiling in drug discovery and development: Perspectives of *in-silico*, *in-vitro* and integrated approaches. *Curr. Drug Metab*, **22**(7): 503–522.

Davies B and Morris T (1993). Physiological parameters in laboratory animals and humans. *Pharm. Res.*, **10**(7): 1093–1095.

de BruynKops C, Sicho M, Mazzolari A and Kirchmair J (2021). GLORYx: Prediction of the metabolites resulting from phase 1 and phase 2 biotransformations of xenobiotics. *Chem. Res. Toxicol*, **34**(2): 286–299.

Garcia-Gonzalez A, Espinosa-Cabello JM, Cerrillo I, Montero-Romero E, Rivas-Melo JJ, Romero-Baez A, Jimenez-Andreu MD, Ruiz-Trillo CA, Rodriguez-Rodriguez A, Martinez-Ortega AJ, Roque-Cuellar MDC, Garcia-Rey S, Jimenez-Sanchez A, Mangas-Cruz MA, Pereira-Cunill JL, Perona JS, Garcia-Luna PP and Castellano JM (2023). Bioavailability and systemic transport of oleanolic acid in humans, formulated as a functional olive oil. *Food Funct.*, **14**(21): 9681–9694.

Genitsaridi I, Salpea P, Salim A, Sajjadi SF, Tomic D, James S, Thirunavukkarasu S, Issaka A, Chen L, Basit A, Luk AOY, Ma RCW, Mbanya JC, Ramachandran A, Wild SH, Duncan BB, Boyko EJ and Magliano DJ (2026). 11th edition of the IDF diabetes atlas: Global, regional and national diabetes prevalence estimates for 2024 and projections for 2050. *Lancet Diabetes Endocrinol.*, **14**(2): 149–156.

Giner-Larza EM, Manez S, Recio MC, Giner RM, Prieto JM, Cerda-Nicolas M and Rios JL (2001). Oleanonic acid, a 3-oxotriterpene from Pistacia, inhibits leukotriene synthesis and has anti-inflammatory activity. *Eur. J. Pharmacol.*, **428**(1): 137–143.

Harley BK, Amponsah IK, Ben IO, Mireku-Gyimah NA, Anokwah D, Neglo D, Amengor CDK and Fleischer TC (2022). Hypoglycaemic activity of Oleanonic acid, a 3-oxotriterpenoid isolated from Aidia Genipiflora (DC.) Dandy, involves inhibition of carbohydrate metabolic enzymes and promotion of glucose uptake. *Biomed. Pharmacother.*, **149**: 112833.

Ichikawa T, Ishida S, Sakiya Y, Sawada Y and Hanano M (1986). Biliary excretion and enterohepatic cycling of

Article in Press

glycyrrhizin in rats. *J. Pharm. Sci.*, **75**(7): 672–675.

Jeong DW, Kim YH, Kim HH, Ji HY, Yoo SD, Choi WR, Lee SM, Han CK and Lee HS (2007). Dose-linear pharmacokinetics of oleanolic acid after intravenous and oral administration in rats. *Biopharm. Drug Dispos.*, **28**(2): 51–57.

Kawabata K, Kitamura K, Irie K, Naruse S, Matsuura T, Uemae T, Taira S, Ohigashi H, Murakami S, Takahashi M, Kaido Y and Kawakami B (2017). Triterpenoids isolated from *Ziziphus jujuba* enhance glucose uptake activity in skeletal muscle cells. *J. Nutr. Sci. Vitaminol*, **63**(3): 193–199.

Khwaza V and Aderibigbe BA (2024). Potential pharmacological properties of triterpene derivatives of ursolic acid. *Molecules*, **29**(16): 3884.

Kostiainen R, Kotiaho T, Kuuranne T and Auriola S (2003). Liquid chromatography/atmospheric pressure ionization-mass spectrometry in drug metabolism studies. *J. Mass Spectrom*, **38**(4): 357–372.

Lipinski CA, Lombardo F, Dominy BW and Feeney PJ (2001). Experimental and computational approaches to estimate solubility and permeability in drug discovery and development settings. *Adv. Drug Deliv. Rev.*, **46**(1–3): 3–26.

Mossi KE, Djalogue L, Djagadou KA, Tchamdja T, Maman S, Apeti S, Nebona L, Gumedzoe E, Balaka A and Djibril MA (2026). Lipid profile of type 2 diabetic patients at sylvanus olympio university hospital in lome. *OPEN J. Endocr. Metab. Dis.*, **16**(1): 1–8.

Mustafa SB, Mehmood Z, Akhter N, Kauser A, Hussain I, Rashid A, Akram M, Tahir IM, Munir N, Riaz M, Niazi SG, Ali A, Ashraf MM, Naz U, Ahmed H, Shah SA and Usmanghani K (2016). Medicinal plants and management of diabetes mellitus: A review. *Pak. J. Pharm, Sci*, **29**: 1885–1891.

Pachi VK, Mikropoulou EV, Gkiouvetidis P, Siafakas K, Argyropoulou A, Angelis A, Mitakou S and Halabalaki M (2020). Traditional uses, phytochemistry and pharmacology of Chios mastic gum (*Pistacia lentiscus* var. Chia, Anacardiaceae): A review. *J. Ethnopharmacol*, **254**: 112485.

Pelletier R, Nahle D, Sarr M, Bourdais A, Morel I, Le Dare B and Gicquel T (2025). Identifying metabolites of new psychoactive substances using *in-silico* prediction tools. *Arch. Toxicol.*, **99**(7): 2953–2973.

Rali S, Oyedeji OO, Aremu OO, Oyedeji AO and Nkeh-Chungag BN (2016). Semisynthesis of derivatives of oleanolic acid from *Syzygium aromaticum* and their antinociceptive and anti-inflammatory properties. *Mediators Inflamm.*, **2016**: 1–9.

Ren C, Kong D, Ning C, Xing H, Cheng Y, Zhang Y, Lu Y, Li N, Chen X and Zhao D (2021). Improved pharmacokinetic characteristics of ursolic acid in rats following intratracheal instillation and nose-only inhalation exposure. *J. Pharm. Sci.*, **110**(2): 905–913.

Similie D, Minda D, Bora L, Kroskins V, Luginina J, Turks M, Dehelean CA and Danciu C (2024). An update on pentacyclic triterpenoids ursolic and oleanolic acids and related derivatives as anticancer candidates. *Antioxidants*, **13**(8): 952–987.

Takahashi M, Izumi Y, Iwahashi F, Nakayama Y, Iwakoshi M, Nakao M, Yamato S, Fukusaki E and Bamba T (2018). Highly accurate detection and identification methodology of xenobiotic metabolites using stable isotope labeling, data mining techniques and time-dependent profiling based on LC/HRMS/MS. *Anal. Chem.*, **90**(15): 9068–9076.

Talbot K, Wang HY, Kazi H, Han LY, Bakshi KP, Stucky A, Fuino RL, Kawaguchi KR, Samoyedny AJ, Wilson RS, Arvanitakis Z, Schneider JA, Wolf BA, Bennett DA, Trojanowski JQ and Arnold SE (2012). Demonstrated brain insulin resistance in alzheimer's disease patients is associated with IGF-1 resistance, IRS-1 dysregulation and cognitive decline. *J. Clin. Invest.*, **122**(4): 1316–1338.

Uddin J, Muhsinah AB, Imran M, Khan MN and Musharraf SG (2022). Structure-fragmentation study of pentacyclic triterpenoids using electrospray ionization quadrupole time-of-flight tandem mass spectrometry (ESI-QTOFMS/MS). *Rapid. Commun. Mass Spectrom*, **36**(4): e9243.

Vasconcelos T, Sarmento B and Costa P (2007). Solid dispersions as strategy to improve oral bioavailability of poor water soluble drugs. *Drug Discov. Today*, **12**(23–24): 1068–1075.

Xi J, Chang Q, Chan CK, Meng ZY, Wang GN, Sun JB, Wang YT, Tong HHY and Zheng Y (2009). Formulation development and bioavailability evaluation of a self-nanoemulsified drug delivery system of oleanolic acid. *AAPS PharmSciTech*, **10**(1): 172–182.

Yang X, Gandhi YA, Duignan DB and Morris ME (2009). Prediction of biliary excretion in rats and humans using molecular weight and quantitative structure–pharmacokinetic relationships. *AAPS J.*, **11**(3): 511–525.

Article in Press